How to cite: *Angew. Chem. Int. Ed.* **2023**, *62*, e202303580
doi.org/10.1002/anie.202303580

Nitrides

Combining MN_6 Octahedra and PN_5 Trigonal Bipyramids in the Mica-like Nitridophosphates MP_6N_{11} (M = Al, In)

*Sebastian J. Ambach, Monika Pointner, Sophie Falkai, Carsten Paulmann, Oliver Oeckler, and Wolfgang Schnick**

Abstract: Layered silicates are a very versatile class of materials with high importance to humanity. The new nitridophosphates MP_6N_{11} (M = Al, In), synthesized from MCl_3, P_3N_5 and NH_4N_3 in a high-pressure high-temperature reaction at 1100 °C and 8 GPa, show a mica-like layer setup and feature rare nitrogen coordination motifs. The crystal structure of AlP_6N_{11} was elucidated from synchrotron single-crystal diffraction data (space group *Cm* (no. 8), a = 4.9354(10), b = 8.1608(16), c = 9.0401(18) Å, β = 98.63(3)°), enabling Rietveld refinement of isotypic InP_6N_{11}. It is built up from layers of PN_4 tetrahedra, PN_5 trigonal bipyramids and MN_6 octahedra. PN_5 trigonal bipyramids have been reported only once and MN_6 octahedra are sparsely found in the literature. AlP_6N_{11} was further characterized by energy-dispersive X-ray (EDX), IR and NMR spectroscopy. Despite the vast amount of known layered silicates, there is no isostructural compound to MP_6N_{11} as yet.

Naturally abundant (oxo)silicates dominate the solid earth crust with a volume fraction of more than 90 %.[1] Despite the limited number of primary building units of the Si/O-networks, predominantly SiO_4 tetrahedra, this class features an immense structural diversity. This includes isolated tetrahedra or small groups thereof, ribbons, layers and 3D-frameworks. Layered silicate structures often consist of stacked SiO_4 tetrahedral (T) and MO_6 (M = Al, Mg, Fe, …) octahedral (O) layers and various cations between oxide layers. Layer stacking between cations usually occurs in two ways: T–O or T–O–T, the latter being typical for micas, a subgroup of layered silicates. Combining these possibilities leads to a large structural variety and a similarly broad field of application, such as ceramics, building materials, (photo)catalysis, adsorbents, feed additives or biomedical applications.[2–10] Furthermore, clay minerals have even been discussed to play an important role in the origin of life.[11,12] The structural limitation of oxygen, usually connecting only up to two tetrahedral centers, is overcome when O is formally replaced by N and Si by P, leading to the class of nitridophosphates. Due to the isoelectronic combination Si/O and P/N, both form similar structural elements, however, with one key difference: In nitridophosphates, N has the possibility to regularly connect up to three tetrahedral P centers, enabling an even larger structural diversity.[13] Occasionally, even edge-sharing PN_4 tetrahedra have been reported (e.g. in α-P_3N_5, α-HP_4N_7 or P_4ON_6). In contrast, edge-sharing SiO_4 tetrahedra have only claimed once, namely for fibrous silica.[14–17] This suggests a plethora of layered silicate minerals isostructural with or closely related to nitridophosphates. However, so far only one such example is known, namely $AESi_3P_4N_{10}(NH)_2$ (AE = Mg, Ca, Sr).[18]

Nitridophosphates are versatile materials, ranging from semiconductors or luminescent materials (when doped with Eu^{2+}) to flame-retardants, safety materials in pyrotechnics, ion conductors or gas storage materials.[19–26] Extending their crystal chemistry in analogy to the manifold structural possibilities of layered silicates, their field of application would widely increase.

In contrast to naturally abundant (oxo)silicates, nitridophosphates are a purely synthetic class of materials. One reason for this is their susceptibility to irreversible thermal decomposition, releasing molecular nitrogen. For their formation, however, often temperatures way above the point of decomposition are necessary. Following Le Chatelier's principle, applying pressure prevents the formation of N_2 and allows high-temperature syntheses to be carried out. Typically, high pressure also affects coordination numbers, increasing the usual fourfold coordination in PN_4 tetrahedra. Thereby, PN_5-pyramids, either square-based in γ-P_3N_5, or trigonal-bipyramidal in γ-HP_4N_7 were observed and even PN_6-octahedra in β-BP_3N_6 could be enforced recently by applying a pressure of 46 GPa.[27–30]

In this contribution, we report on the highly condensed nitridophosphates MP_6N_{11} (M = Al, In), which adopt a mica-like structure with rare coordination motifs. The title compounds were synthesized in a high-pressure high-

[*] S. J. Ambach, M. Pointner, S. Falkai, Prof. Dr. W. Schnick
Department of Chemistry, University of Munich (LMU)
Butenandtstraße 5–13, 81377 Munich (Germany)
E-mail: wolfgang.schnick@uni-muenchen.de
Dr. C. Paulmann
Institute for Mineralogy, Crystallography and Petrography, University of Hamburg
Grindelallee 48, 20146 Hamburg (Germany)
Prof. Dr. O. Oeckler
Faculty of Chemistry and Mineralogy, Leipzig University
Scharnhorststraße 20, 04275 Leipzig (Germany)

temperature reaction at 8 GPa and 1100 °C starting from MCl_3, P_3N_5 and NH_4N_3 (equation 1). Starting materials were ground in a glove box under an argon atmosphere, tightly packed into a h-BN crucible and reacted in a multianvil press.[31] Further details on the synthesis are given in the Supporting Information.

$$4\,MCl_3 + 8\,P_3N_5 + 3\,NH_4N_3 \rightarrow 4\,MP_6N_{11} + 12\,HCl + 4\,N_2 \quad (1)$$

The reactions yielded a gray, microcrystalline powder, which is stable at ambient conditions. In both cases, best yields were obtained using only 10 % of the required stoichiometric amount of NH_4N_3. Without this significant deviation from the ideal stoichiometry, diverse unknown side phases are formed, presumably containing H due to the high partial pressure of HCl. The in situ generated HCl seems to act as a mineralizer enhancing single-crystal growth, as it is known for the ability to reversibly cleave P–N bonds.[32] Thereby plate-shaped single crystals of AlP_6N_{11} up to $70\times70\ \mu m^2$ in length and width (Figure 1) were obtained. In contrast, InP_6N_{11} forms small acicular single crystals that are only up to two µm long.

MP_6N_{11} (M = Al, In) can be interpreted as the formal reaction product of MN and P_3N_5 in a molar ratio of 1:2. A direct high-pressure high-temperature reaction of these compounds, however, does not yield MP_6N_{11}. Instead, MN results as the main crystalline constituent alongside minor unknown phases and an amorphous portion, which the higher reactivity of MCl_3 compared to MN may explain. Coherent with this, the synthesis of analogous GaP_6N_{11} was not possible as yet. With the required usage of $GaCl_3$, the powder mixture starts to react with the boron nitride crucible and forms BP_3N_6 as the only crystalline product.[30]

The crystal structure of AlP_6N_{11} was elucidated from synchrotron single-crystal X-ray diffraction data (space group Cm (no. 8), a = 4.9354(10), b = 8.1608(16), c = 9.0401(18) Å, β = 98.63(3)°).[33] The data were collected at beamline P24 at DESY (Hamburg, Germany; more information in the Supporting Information). The elemental compositions of both title compounds were analyzed by energy-dispersive X-ray (EDX) spectroscopy (Tables S2 and S3). In the respective samples, MP_6N_{11} was confirmed as the main crystalline constituent by Rietveld refinement (Figures S2 and S3).

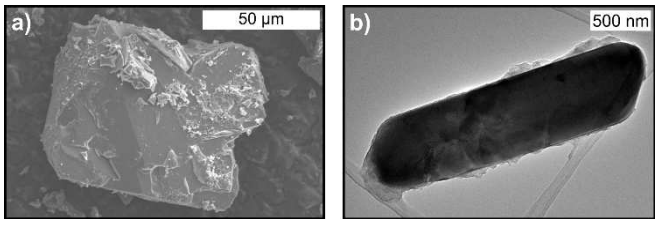

Figure 1. Exemplary a) scanning electron microscope (SEM) image of a plate-shaped single crystal of AlP_6N_{11} and b) transmission electron microscope (TEM) image of a small needle-shaped crystallite of InP_6N_{11}.

The layered structure of AlP_6N_{11} is built up from AlN_6 octahedra, PN_4 tetrahedra and PN_5 trigonal bipyramids (Figures 2 and 3). The AlN_6 octahedra are not interconnected, while both PN_4 tetrahedra and PN_5 trigonal bipyramids form *sechser* rings, as defined by Liebau.[1] A more detailed view on the layered structure is provided in the Supporting Information (Figure S1). This setup is comparable to layered silicates, however, to the best of our knowledge, there is no clay mineral or mica, which is isotypic to MP_6N_{11}, probably because trigonal bipyramids SiO_5 have only been reported for exceptional oxosilicates.[34,35] A related layer sequence is found in the mica clintonite ($Ca(Mg,Al)_3(Al_3Si)O_{10}(OH)_2$), with the exception of $(Al,Si)O_6$ octahedra instead of PN_5 trigonal bipyramids (Figure S1).[36]

The AlN_6 octahedra, rarely found in the literature (e.g. $AlP_6O_{3x}(NH)_{3-x}N_9$ or rock salt-type high-pressure AlN), are significantly elongated along one axis, leading to Al–N bond lengths of 2.056(8) and 2.087(9) Å in the equatorial plane and 2.342(9) and 2.392(10) Å in the axial direction, respectively.[37,38] Typical Al–N distances in octahedral coordination, as found in the aforementioned compounds, vary around 2.0 Å. N–Al–N angles are between 87.5(4) and 92.6(4)° and thus in a typical range for octahedra of ideally

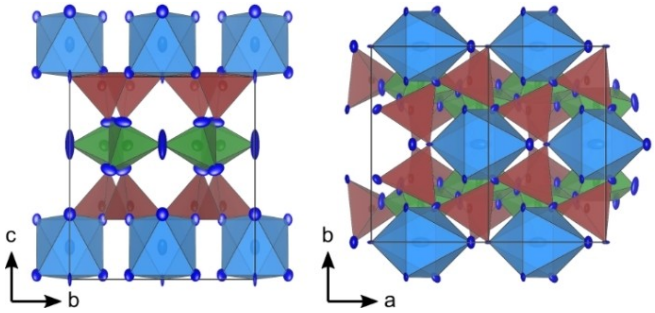

Figure 2. The layered crystal structure of AlP_6N_{11} consists of AlN_6 octahedra (blue), PN_5 trigonal bipyramids (green) and PN_4 tetrahedra (red). Displacement ellipsoids are displayed at 90 % probability level.

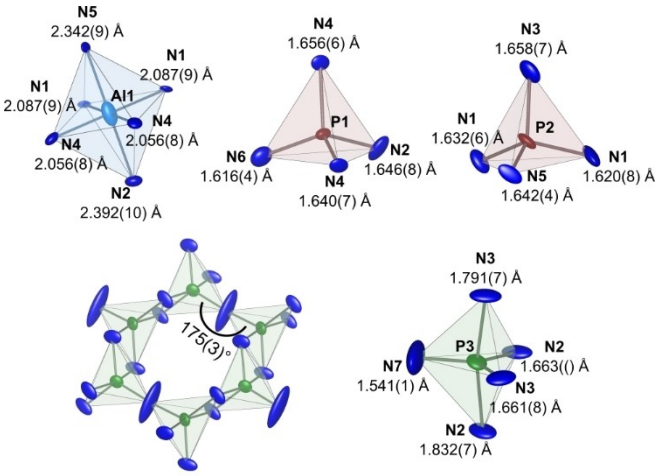

Figure 3. Coordination polyhedra of Al1, P1, P2 and P3 in AlP_6N_{11}.

90°. P–N distances (1.6283(8)–1.6492(11) Å) and N–P–N angles (102.7(4)–122.2(4)°) in the PN_4 tetrahedra can be compared to other nitridophosphates, e.g. P_3N_5 or $AlP_6O_{3x}(NH)_{3-x}N_9$.[12,37] So far, trigonal bipyramidal PN_5 units were only observed in the high-pressure polymorph γ-HP_4N_7, where two longer and three shorter bonds appear.[26] Comparable bond lengths and angles can be observed in AlP_6N_{11}, with 1.832(7) and 1.791(7) Å for the longer and 1.5408(13)–1.663(8) Å for the shorter bonds. As in γ-HP_4N_7, PN_5 units share edges, forming infinite strands along [100], however, with a major difference. While in γ-HP_4N_7 these strands do not interact with each other, they are directly interconnected via the N7 atom in AlP_6N_{11}. This leads to an energetically unfavorable, almost linear coordination (175-(3)°) of N7, resulting in a large thermal displacement ellipsoid with its largest displacement perpendicular to the P3···P3 vector (Figure 3). This feature has not yet been described for nitridophosphates. However, it appears in oxosilicates, e.g. $K_3NdSi_7O_{17}$.[39] Such angles of approximately 180° can be seen as a time and position average rather than an actual bond angle. Its real value, at any instant in time, is likely to be much smaller than 180°. This is also consistent with a small P3–N7 distance of 1.5408(13) Å in case of the almost linear coordination, which would be larger with smaller bond angles. Other comparable bond lengths in trigonal bipyramids show values of 1.661(8) (P3–N3) and 1.663(8) Å (P3–N2). Even at low temperatures (173(2) K) this observation does not change.

The electrostatic plausibility of the crystal structure and polyhedral distortions were analyzed by charge distribution (CHARDI), bond-valence-sum (BVS) and minimal bonding ellipsoid (MBE) calculations, all of which confirm the consistency of the structure model.[41–43] Corresponding results and more detailed information are provided in the Supporting Information (Tables S11 and S12, Figure S9).

Data obtained from X-ray diffraction initially suggest the higher symmetric space group *C*2/*m* (no.12) instead of the chosen *Cm* (no. 8). This, however, would cause two major issues. First, the nitrogen atom connecting the PN_5-strands (N7, Figure 3) is forced into the energetically unfavorable linear coordination with a P3–N7–P3 angle of exactly 180°. Avoiding this by introducing a 50:50 split position of N7 still results in large displacement ellipsoids. Second, a twofold axis would lead to the crystallographic equivalency of all P sites of the PN_4 tetrahedra. This is not consistent with the results of ^{31}P NMR spectroscopy (Figure 4b).

The ^{31}P spectrum shows one signal at $\delta = -130.0$ ppm, corresponding to penta-coordinated P in the PN_5 trigonal bipyramids. A comparable chemical shift was reported for P in γ-HP_4N_7 ($\delta = -103.0$ ppm), which also contains trigonal bipyramidal PN_5 units.[26] Additionally, two signals at $\delta =$ 14.5 and 12.0 ppm are observed, which is a typical range for fourfold N-coordinated P, as observed e.g. in $AlP_6O_{3x}(NH)_{3-x}N_9$.[36] These signals suggest two independent crystallographic P sites for PN_4 tetrahedra, which is met in space group *Cm* but not in *C*2/*m* (only one P site). Whereas X-ray diffraction averages over long distances and may render space group *C*2/*m* acceptable, NMR spectroscopy is sensitive to short-range interactions and rules out *C*2/*m* in the local environment. Thus, we prefer space group *Cm* for the structure model. The measure of similarity, calculated by the COMPSTRU tool of the Bilbao Crystallographic Server, has a value of $\Delta = 0.114$, indicating only small deviations between both structure models.[44–49] For this reason, possible ferroelectric properties caused by the non-centrosymmetric structure would be minimal, if measurable at all. Additionally, a high-temperature phase transition from space group *Cm* to *C*2/*m* could be possible, however would require temperature-dependent solid-state NMR-measurements.

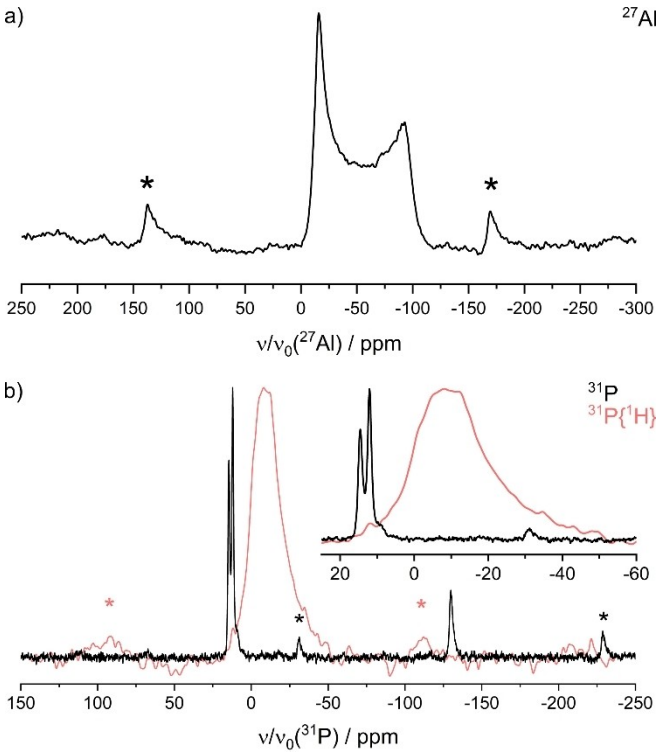

Figure 4. Solid-state MAS NMR spectra of AlP_6N_{11}. a) One signal in the ^{27}Al spectrum. b) Three signals in the ^{31}P (black) and one signal in the ^{31}P{^{1}H} (red) spectra. The number of signals is consistent with the structure model in *Cm*, showing no evidence of H in AlP_6N_{11}. Sidebands are marked with asterisks.

Structure elucidation of AlP_6N_{11} enabled Rietveld refinement (Figure S3) for InP_6N_{11} ($a = 4.9723(2)$, $b = 8.2930(3)$, $c = 9.2627(4)$ Å, $\beta = 99.217(1)$°). In contrast to AlP_6N_{11}, the ^{31}P NMR spectrum of InP_6N_{11} (Figure S5) shows only one signal for tetrahedrally coordinated P ($\delta = 6.8$ ppm). This may be a superposition of two separate signals, leading to space group *Cm*, as in case of AlP_6N_{11}. On the other hand, based on NMR results space group *C*2/*m* is feasible for the structure model of InP_6N_{11}. As we see no apparent reason for a change in space group, we prefer *Cm* for InP_6N_{11} as well. In–N distances of the elongated InN_6 octahedra range from 2.21(7) to 2.29(7) Å in the equatorial plane, comparable to rock salt-type high-pressure InN, and from 2.33(6) to 2.60(5) Å along the axial direction.[40] All bond lengths and angles of the P–N polyhedra are comparable to AlP_6N_{11}.

The *c* lattice parameter is expanded by 2.4 % from 9.0401 (18) Å in AlP_6N_{11} to 9.2627(4) Å in InP_6N_{11}.

To rule out imide functionality in MP_6N_{11} (M = Al, In), which might be introduced by the starting material NH_4N_3 or short contact with air before the synthesis, IR- and solid-state NMR spectra (Figure 4) were recorded. As in the case of $EASi_3P_4N_{12}H_2$ (EA = Mg, Ca, Sr), N–H valence modes are typically observed at around 3400 cm^{-1} in IR-spectra, whereas the spectrum of AlP_6N_{11} shows no such absorption band (Figure S6).[16]

As a much more sensitive probe towards hydrogen, solid-state NMR measurements show the same result. The ^{27}Al (spin $I = {}^5/_2$) spectrum shows one broad signal between $\delta = 0$ and -100 ppm, which is in line with one crystallographic Al site. The shift is comparable to octahedrally coordinated Al as reported in the literature.[36,50] The signal of the $^{31}P\{^1H\}$ cross polarized spectrum does not match any positions of the signals in the direct ^{31}P spectrum, indicating the absence of hydrogen in AlP_6N_{11}. The broad signal in the $^{31}P\{^1H\}$ cross polarized spectrum may be explained by a minor amorphous side phase, containing both P and H. The ^1H NMR and all other NMR spectra of AlP_6N_{11} can be found in the Supporting Information (Figure S4).

Despite the thermal sensitivity of many nitridophosphates, AlP_6N_{11} is stable up to at least 950 °C under argon atmosphere (Figure S7) and shows a thermal volume expansion of 16.0 ppm/K, which is small compared to silicate clay minerals and micas.[51,52] In the former, the lattice parameter perpendicular to the layers usually shows a much higher thermal expansion than the ones parallel to the layers. In AlP_6N_{11}, however, the increase in volume is caused by the expansion of the lattice parameter perpendicular to the layers and only one lattice parameter parallel to the layers. The second parallel lattice parameter only shows a very small increase in length. (Figure S8) This behavior may be a feature of the nearly linear coordinated N7 atom (Figure 3). Upon expansion along [010], the P3–N7–P3 angle would be further stretched towards the energetically unfavorable value of 180°.

Summing up, we synthesized the mica-analogous nitridophosphates MP_6N_{11} (M = Al, In), which contain the rare structure motifs of MN_6 octahedra and PN_5 trigonal bipyramids. As the second nitridic compound structurally mimicking layered silicate minerals, this gives proof that nitridophosphates should systematically be able to adopt structures of the former and $AESi_3P_4N_{10}(NH)_2$ (AE = Mg, Ca, Sr) is not just a stand-out curiosity. Exploring nitridic analogs of layered silicate minerals, with the aim to expand the already wide variety of structures and applications of nitridophosphates, seems an intriguing approach for further studies. Targeting compositions and structures known from nature promises to yield a vast amount of new nitridophosphates with applications as essential as the ones of silicate clay minerals and micas.

Acknowledgements

We gratefully acknowledge the financial support by Deutsche Forschungsgemeinschaft (projects SCHN 377/18-1 and OE530/6-1). The Deutsches Elektronensynchrotron (DESY, Hamburg) is acknowledged for granting beamtime (project I-20210953). Laetitia Bradaczek, Alexander Feige, Niklas Langer and Lennart Staab are acknowledged for help during the beam time. Furthermore, the authors thank Christian Minke and Amalina Buda for the SEM and EDX measurements as well as solid-state NMR experiments. Open Access funding enabled and organized by Projekt DEAL.

Conflict of Interest

The authors declare no conflict of interest.

Data Availability Statement

The data that support the findings of this study are available in the supplementary material of this article.

Keywords: Aluminum · High-Pressure Chemistry · Layered Structures · Nitrides · Nitridophosphate

[1] F. Liebau in *Structural Chemistry of Silicates. Structure, Bonding, and Classification*, Springer, Berlin, Heidelberg, **1985**, pp. 212–229. The term *"sechser ring"* has been defined by Liebau and is derived from the German word "sechs" (engl. six), describing a ring formed by six polyhedra.
[2] F. Bergaya, G. Lagaly in *Handbook of Clay Science, Vol. 2*, Elsevier, Amsterdam, **2006**, pp. 1–19.
[3] H. H. Murray, *Appl. Clay Sci.* **1991**, *5*, 379–395.
[4] M. Valásková, *Ceram.-Silik.* **2015**, *59*, 331–340.
[5] M. Ghadiri, W. Chrzanowski, R. Rohanizadeh, *RSC Adv.* **2015**, *5*, 29467–29481.
[6] Y. Zou, Y. Hu, Z. Shen, L. Yao, D. Tang, S. Zhang, S. Wang, B. Hu, G. Zhao, X. Wang, *J. Environ. Sci.* **2022**, *115*, 190–214.
[7] W. D. Johns, *Annu. Rev. Earth Planet. Sci.* **1979**, *7*, 183–198.
[8] C. H. Zhou, J. Keeling, *Appl. Clay Sci.* **2013**, *74*, 3–9.
[9] M. Nadziakiewicza, S. Kehoe, P. Micek, *Animal* **2019**, *9*, 714.
[10] V. Reyes-Zamudio, C. Angeles-Chávez, J. Cervantes, *J. Therm. Anal. Calorim.* **2011**, *104*, 405–413.
[11] A. Weiss, *Angew. Chem. Int. Ed. Engl.* **1981**, *20*, 850–860.
[12] J. T. Kloprogge, H. Hartmann, *Life* **2022**, *12*, 259–313.
[13] S. D. Kloß, W. Schnick, *Angew. Chem. Int. Ed.* **2019**, *58*, 7933–7944.
[14] S. Horstmann, E. Irran, W. Schnick, *Angew. Chem. Int. Ed. Engl.* **1997**, *36*, 1873–1875.
[15] S. Horstmann, E. Irran, W. Schnick, *Angew. Chem. Int. Ed. Engl.* **1997**, *36*, 1992–1994.
[16] J. Ronis, B. Bondars, A. Vitola, T. Millers, J. Schneider, F. Frey, *J. Solid State Chem.* **1995**, *115*, 265–269.
[17] A. Weiss, A. Weiss, *Z. Anorg. Allg. Chem.* **1954**, *276*, 95–112.
[18] L. Eisenburger, P. Strobel, P. J. Schmidt, T. Bräuniger, J. Wright, E. L. Bright, C. Giacobbe, O. Oeckler, W. Schnick, *Angew. Chem. Int. Ed.* **2022**, *61*, e202114902.
[19] Y. Hirota, T. Kobayashi, *J. Appl. Phys.* **1982**, *53*, 5037–5043.
[20] Y.-H. Jeong, K.-H. Choi, S.-K. Jo, B. K. Bongkoo Kang, *Jpn. J. Appl. Phys.* **1995**, *34*, 1176–1180.

[21] F. J. Pucher, A. Marchuk, P. J. Schmidt, D. Wiechert, W. Schnick, *Chem. Eur. J.* **2015**, *21*, 6443–6448.
[22] S. Wendl, L. Eisenburger, P. Strobel, D. Günther, J. P. Wright, P. J. Schmidt, O. Oeckler, W. Schnick, *Chem. Eur. J.* **2020**, *26*, 7292–7298.
[23] M. S. Choudhary, J. K. Fink, K. Lederer, H. A. Krässig, *J. Appl. Polym. Sci.* **1987**, *34*, 863–869.
[24] E.-C. Koch, S. Cudziło, *Angew. Chem. Int. Ed.* **2016**, *55*, 15439–15442.
[25] W. Schnick, J. Luecke, *Solid State Ionics* **1990**, *38*, 271–273.
[26] F. Karau, W. Schnick, *Angew. Chem. Int. Ed.* **2006**, *45*, 4505–4508.
[27] K. Landskron, H. Huppertz, J. Senker, W. Schnick, *Angew. Chem. Int. Ed.* **2001**, *40*, 2643–2645.
[28] D. Baumann, W. Schnick, *Angew. Chem. Int. Ed.* **2014**, *53*, 14490–14493.
[29] S. Vogel, M. Bykov, E. Bykova, S. Wendl, S. D. Kloß, A. Pakhomova, S. Chariton, E. Koemets, N. Dubrovinskaia, L. Dubrovinsky, W. Schnick, *Angew. Chem. Int. Ed.* **2019**, *58*, 9060–9063.
[30] K. Landskron, H. Huppertz, J. Senker, W. Schnick, *Z. Anorg. Allg. Chem.* **2002**, *628*, 1465–1471.
[31] H. Huppertz, *Z. Kristallogr. - Cryst. Mater.* **2004**, *219*, 330–338.
[32] S. Vogel, A. T. Buda, W. Schnick, *Angew. Chem. Int. Ed.* **2018**, *57*, 13202–13205.
[33] Deposition number 2241809 contains the supplementary crystallographic data for this paper. These data are provided free of charge by the joint Cambridge Crystallographic Data Centre and Fachinformationszentrum Karlsruhe Access Structures service.
[34] A. Pakhomova, E. Bykova, M. Bykov, K. Glazyrin, B. Gasharova, H.-P. Liermann, M. Mezouar, L. Gorelova, S. Krivovichev, L. Dubrovinsky, *IUCrJ* **2017**, *4*, 671–677.
[35] F. Liebau, *Inorg. Chim. Acta* **1984**, *89*, 1–7.
[36] J. A. MacKinney, C. I. Mora, S. W. Bailey, *Am. Mineral.* **1988**, *73*, 365–375.
[37] L. Neudert, F. Heinke, T. Bräuniger, F. J. Pucher, G. B. Vaughan, O. Oeckler, W. Schnick, *Chem. Commun.* **2017**, *53*, 2709–2712.
[38] H. Vollstädt, E. Ito, M. Akaishi, S. Akimoto, O. Fukunaga, *Proc. Jpn. Acad. Ser. B* **1990**, *66*, 7–9.
[39] S. M. Haile, B. J. Wuensch, *Acta Crystallogr. Sect. B* **2000**, *56*, 773–779.
[40] M. Ueno, M. Yoshida, A. Onodera, O. Shimomura, K. Takemura, *Phys. Rev. B: Condens. Matter Mater. Phys.* **1994**, *49*, 14–21.
[41] K. Momma, F. Izumi, *J. Appl. Crystallogr.* **2011**, *44*, 1272–1276.
[42] A. S. Wills, VaList - A bond valence calculation and analysis program, London, **2010**.
[43] J. Cumby, J. P. Attfield, *Nat. Commun.* **2017**, *8*, 14235.
[44] G. Bergerhoff, M. Berndt, K. Brandenburg, T. Degen, *Acta Crystallogr. Sect. B* **1999**, *55*, 147–156.
[45] M. I. Aroyo, J. M. Perez-Mato, D. Orobengoa, E. Tasci, G. de la Flor, A. Kirov, *Bulg. Chem. Commun.* **2011**, *43*, 183–197.
[46] M. I. Aroyo, J. M. Perez-Mato, C. Capillas, E. Kroumova, S. Ivantchev, G. Madariaga, A. Kirov, H. Wondratschek, *Z. Kristallogr.* **2006**, *221*, 15–27.
[47] M. I. Aroyo, A. Kirov, C. Capillas, J. M. Perez-Mato, H. Wondratschek, *Acta Crystallogr. Sect. A* **2006**, *62*, 115–128.
[48] G. de la Flor, D. Orobengoa, E. Tasci, J. M. Perez-Mato, M. I. Aroyo, *J. Appl. Crystallogr.* **2016**, *49*, 653–664.
[49] E. S. Tasci, G. de la Flor, D. Orobengoa, C. Capillas, J. M. Perez-Mato, M. I. Aroyo, *EPJ Web Conf.* **2012**, *22*, 00009.
[50] T. Bräuniger, M. Jansen, *Z. Anorg. Allg. Chem.* **2013**, *639*, 857–879.
[51] H. A. McKinstry, *Am. Mineral.* **1965**, *50*, 212–222.
[52] M. Gemmi, M. Merlini, A. Pavese, N. Curetti, *Phys. Chem. Miner.* **2008**, *35*, 367–379.

Manuscript received: March 10, 2023
Accepted manuscript online: April 13, 2023
Version of record online: May 4, 2023